Multi-feature based network revealing the structural abnormalities in autism spectrum disorder

Weihao Zheng, *Member*, *IEEE*, Tehila Eilam-Stock, Tingting Wu, Alfredo Spagna, Chao Chen, Bin Hu*, *Member, IEEE,* and Jin Fan*

Abstract—Autism spectrum disorder (ASD) is accompanied with impaired social-emotional functioning, such as emotional regulation and recognition, communication, and related behavior. Study of the alternations of the brain networks in ASD may not only help us in understanding this disorder but also inform us the mechanisms of affective computing in the brain. Although morphological features have been used in the diagnosis of a variety of neurological and psychiatric disorders, these features did not show significant discriminative value in identifying patients with ASD, possibly due to the omission of the information related to the changes in structural similarities among cortical regions. In this study, structural images from 66 high-functioning adults with ASD and 66 matched typically-developing controls (TDC) were used to test the hypothesis of cortico-cortical relationships are abnormal in ASD. Seven morphological features of each of the 360 brain regions were extracted and elastic network was used to quantify the similarities between each target region and all other regions. The similarities were then used to construct multi-feature-based networks (MFN), which were then submitted to a support vector machine classifier to classify the individuals of the two groups. Results showed that the classifier with features of MFN significantly improved the accuracy of discriminating patients with ASD from TDCs (78.63%) compared to using morphological features only (< 65%). The combination of MFN features with morphological features and other high-level MFN properties did not further enhance the classification performance. Our findings demonstrate that the variations in cortico-cortical similarities are important in the etiology of ASD and can be used as biomarkers in the diagnostic process.

Index Terms—Autism Spectrum Disorder (ASD), social-emotional functioning, multi-feature-based network (MFN), diagnostic biomarker

1 INTRODUCTION

AUTISM Spectrum Disorder (ASD) is a pervasive neurodevelopmental condition affecting emotion, cognition and behavior throughout the lifespan. The core symptoms of ASD include abnormal emotional regulation and social interactions, restricted interest, repetitive behaviors and hypo-or-hyper reactivity to sensory stimuli [1, 2]. According to current estimates, between 0.5-2% of the population is affected by ASD [3-5]. Currently, the main method for diagnosis is an extensive clinical evaluation, usually performed by psychologists and psychiatrists utilizing validated diagnostic tools such as the Autism Diagnosis Observation Schedule (ADOS) [6] and the Autism Diagnostic Interview – Revised (ADI-R) [7]. Because ASD is indicated by significant alterations in cerebral morphology compared to typically-developing controls (TDC), e.g., overgrowth of frontal cortex in early childhood (Courchesne, et al., 2003; Hazlett, et al., 2017; Zwaigenbaum, et al., 2014), age-related variation in cortical thickness (CT) (Raznahan, et al., 2009; Wallace, et al., 2010), and abnormalities in grey matter (GM) structures in both childhood and adulthood [8-11], the magnetic resonance imaging (MRI) based diagnosis should have large application value. However, such applications currently have a limited accuracy [12-14]. Therefore, development of sophisticated analytic methods and a deep understanding of the neuromorphological underpinning of ASD are essential.

Recent studies using multiple morphological measures and machine learning technologies to differentiate ASD from TDC have reported remarkable classification accuracies on small sample sets (20 – 30 subjects) based on anatomical features, such as GM density [15, 16] and geometric and/or volumetric features of cortical surface [17-19]. However, these morphological measures produced near-chance accuracy (~60%) when used on large heterogeneous datasets [12, 14]. These results suggest that structural abnormalities of individual brain regions may not provide sufficient information for diagnostic purposes or may underrepresent potential brain mechanisms of ASD. Recently, structural similarity between paired brain regions have achieved marked per-

- *W. Zheng and B. Hu are with School of Information Science and Engineering, Lanzhou University, Lanzhou, P.R. China 730000.*
- *T. Eilam-Stock, T. Wu, and J. Fan are with Department of Psychology, Queens College, City University of New York, New York, NY 11367, USA*
- *T. Eilamstock and J. Fan are also with the Icahn School of Medicine at Mount Sinai, New York, USA.*
- *A. Spagna is with Department of Psychology, Columbia University, New York, USA.*
- *C. Chen is with Department of Biomedical Informatics, Stony Brook University, Stony Brook, USA.*

*Please note that all acknowledgments should be placed at the end of the paper, before the bibliography (**note that corresponding authorship is not noted in affiliation box, but in acknowledgment section**).*

TABLE 1
DEMOGRAPHIC INFORMATION OF PARTICIPANTS

Group	Gender (M/F)		Age			Full scale IQ		
	TDC	ASD	TDC	ASD	*p*	TDC	ASD	*p*
SBL	15/0	15/0	34(7)	35(10)	0.69	-	-	-
KUL	14/0	14/0	23(3)	22(4)	0.28	113(10)	109(13)	0.48
NYU	15/4	15/4	25(5)	25(6)	0.81	113(12)	108(13)	0.25
ISMMS	16/2	16/2	28(7)	28(6)	0.86	117(15)	111(17)	0.22
Total	60/6	60/6	27(7)	27(8)	0.99	114(12)	110(14)	0.90

NYU = New York University Langone Medical Center; SBL = Social Brain Lab at the Research School of Behavioral and Cognitive Neurosciences, University Medical Center Groeningen and Netherlands Institute for Neurosciences; KUL = Katholieke Universiteit Leuven; ISMMS = Icahn School of Medicine at Mount Sinai; TDC = typically-developed controls; ASD = autism spectrum disorder; M/F = male/female; Age and IQ are shown as mean (standard deviation); the two cohorts did not significantly differ in age and in IQ.

formance for identifying Alzheimer's disease [20, 21], fragile X syndrome [22], and children with ASD [19]. However, it is still unclear whether the cortico-cortical relationship is different in adults with ASD, along with its application value for diagnostic purposes.

To test our hypothesis of abnormalities in cortico-cortical similarity of high-functioning adults with ASD, we quantified the inter-regional similarity by using Elastic Network [23] based on seven morphological measures extracted from individuals' brain images [24-29]. This method was shown to be a valid statistical method to establish a relational network based on multi-dimensional features [30] and is robust for estimating network when the number of brain regions is larger than sample size [31]. We then built a multi-feature-based network (MFN) [32] for each individual and examined its classification performance using support vector machine (SVM) [33] with leave-one-out cross validation strategy. The comparisons in terms of classification performances between vertex-based morphological features, voxel-based GM density, MFN, as well as network properties of MFN were conducted to demonstrate the significant improvement in classification and to support the hypothesis that ASD is associated with the changes in the relationship among brain regions in terms of morphological features.

2 MATERIALS AND METHODS

2.1 Imaging Data

Structural brain images were acquired from the ABIDE database (http://fcon_1000.projects.nitrc.org/indi/abide). The structural brain scans of 66 adults with ASD and 66 matched TDCs selected from 4 independent study sites (New York University Langone Medical Center: NYU; Social Brain Lab at the Research School of Behavioral and Cognitive Neurosciences, University Medical Center Groeningen and Netherlands Institute for Neurosciences: SBL; Katholieke Universiteit Leuven: KUL; Icahn School of Medicine at Mount Sinai: ISMMS) were the same as in our previous study [10]. Patients with ASD were all in the high-functioning end of the spectrum (IQ > 80), and received a clinician's DSM-IV-TR diagnosis of Autistic Disorder, Asperger's Disorder, or Pervasive Developmental Disorder Not-Otherwise-Specified. The two groups were matched on gender, age, and full scale IQ for each sites and cross sites ($t(130) = 0.2$; $p = .99$ for age and $t(112) = 1.7$; $p = 0.90$ for full scale IQ). Descriptive data for the samples are shown in Table 1. Although the information of full scale IQ of SBL dataset were not available, all participants received full scale IQ tests and their scores were within the normal range.

2.2 Image Preprocessing

All image data were processed using FreeSurfer v5.3.0 (http://surfer.nmr.mgh.harvard.edu). Briefly, preprocessing included motion correction, removal of non-brain tissue [34], Talairach transformation, intensity normalization, segmentation, and generation of grey-white matter boundary [35]. Topology and geometry of the reconstructed surface were validated once the cortical surface reconstruction was completed [36]. Surfaces were inflated and registered to a priori template by which regional averages of cortical thickness (CT), surface area (SA), cortical volume (CV), local gyrification index (LGI), sulcal depth (SD), gyri height (GH) and curvature (CURV) were calculated. One ASD participant was excluded because the folding information could not be extracted. Both unsmoothed images and smoothed images using a 10-mm full-width-of-half-maximum Gaussian kernel were examined.

For comparison with GM density, VBM analyses were conducted using the CAT12 toolbox (www.neuro.uni-jena.de/cat12/CAT12-Manual.pdf) in Statistical Parametric Mapping (SPM12) with the default setting. Briefly, T1 images were normalized using affine, followed by intra-subject realignment, bias correction for homogeneities, and the segmentation of GM, white matter and cerebral spinal fluid (CSF) [37]. The DARTEL algorithm [38] was applied to the segmented GM images for spatial normalization, and for resampling of image to a 3 × 3 × 3 mm spatial resolution. Non-linear deformation for the effect of spatial normalization was corrected to generate these modulated normalized images, which represent relative volume after correcting for brain size. Each image was then smoothed using an 8-mm full width at half maximum Gaussian kernel.

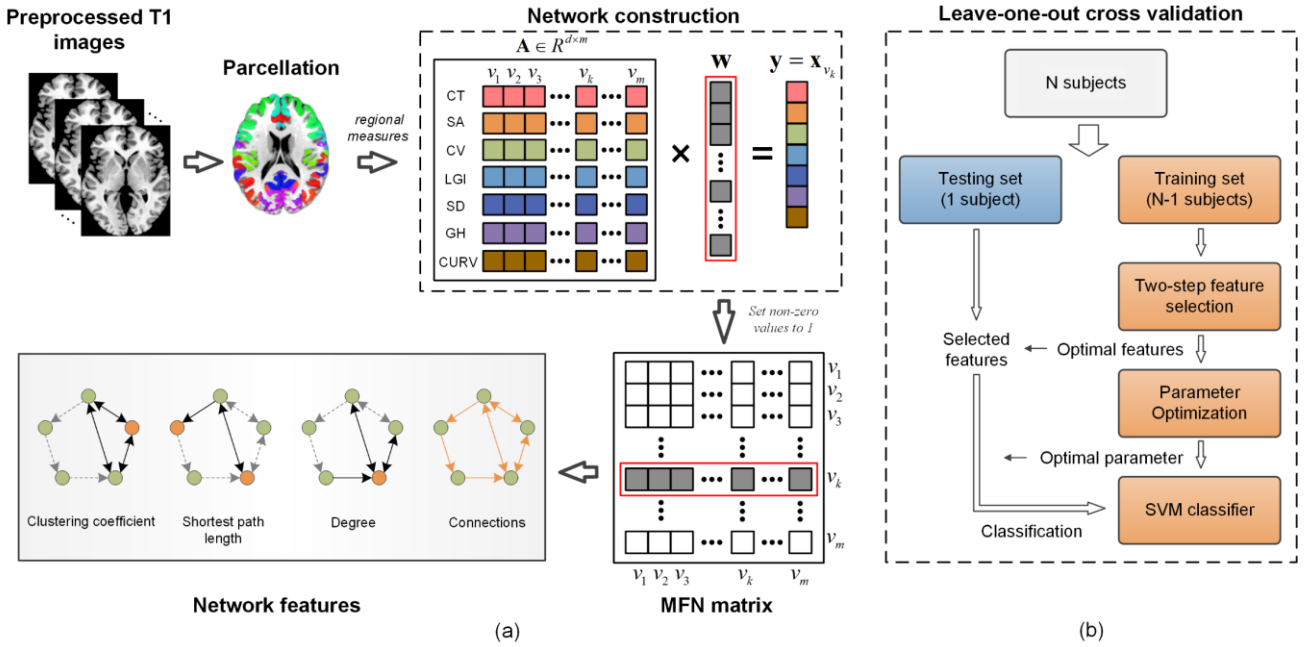

Fig. 1. Schematic representation of multi-feature based network (MFN) construction pipeline (a) and leave-one-out cross-validation process (b). The pipeline of MFN construction. Seven types of morphological features were extracted and averaged within each of the 358 brain regions based on a priori parcellation. The averaged features were concatenated to an m×1 vector for each region, and elastic network was utilized to quantify the cortico-cortical relationship between the vector of one brain region (the target variable, **y**) and the vectors of other regions (the regressors, **A**). The regression process was repeated 358 times. An example of the *k*-th regression process is also given by using a parcellation with m nodes (v_1 - v_m), in which **y** is the feature vector of region v_k. The *k*-th row in the network matrix represents a set of regression coefficients (**W**) from a sparse regression model (nonzero values were set to 1). Connections and properties of the established network were used for classification. The leave-one-out cross-validation process with nested feature selection, parameter optimization and SVM classifier.

2.3 Construction of Multi-feature-based Network (MFN)

For network construction, nodes were the regions defined by the brain parcellation with 360 cortical regions and without subcortical tissues [39]. The hippocampus was excluded from this analysis due to inability to extract folding information from this region. Thus, a total of 358 cortical regions of the entire brain were included.

For edges of the network, Elastic Net [23] was utilized instead of paired correlations (e.g., Pearson correlation), to quantify the relationship between the target brain region and multiple predictor regions. During each regression process, the L1-norm regularization was used to obtain a sparse solution that efficiently excluded the irrelevant predictors [40], and L2-norm regularization was used to compensate for the deficits of L1-norm regularization that L1-norm regularization only identifies the number of predictors that equal to the number of observations and only selects one from the highly correlated predictors [23].

For the calculation of the edges, we denote each individual as $\mathbf{X} = [x_1, x_2, ..., x_m]^T \in R^{m \times d}$, with total m brain regions and d morphological features (7 features in our analysis) of each region. Each regional morphological feature of an individual was normalized using the global average and the standard deviation of this feature. The cortico-cortical relationships were generated by multiple regression procedure, with each brain region alternately serving as the target region and the remaining regions as the predictors. For example, in the *i*-th regression, x_i was regarded as the target vector, and the other *m*-1 regional vectors could form the regressor matrix **A**. Therefore, we set the x_i in **A** to 0 ($\mathbf{A} = [x_1, x_2, ..., x_{i-1}, 0, x_{i+1}, ..., x_m]$), denoted a regressor matrix including all regional vectors except the *i*-th region. The linear regression model was defined as $\mathbf{y} = \mathbf{Aw}$, where $\mathbf{w} \in R^{m \times 1}$ and **y** denoted the regression coefficient vector and target vector, respectively. The sparse solution was realized by solving the regularized optimization problem, formulated as:

$$\min_{\mathbf{w}} \frac{1}{2} \|\mathbf{y} - \mathbf{Aw}\|_2^2 + \lambda_1 \|\mathbf{w}\|_1 + \lambda_2 \|\mathbf{w}\|_2^2 \quad (1)$$

where λ_1 is the sparsity control parameter, with a larger value indicating a sparser regression coefficient vector. Non-zero values in the achieved sparse coefficient vector were set to 1. Finally, an MFN matrix (358 × 358) was formed by using the obtained binary coefficient vectors. The SLEP package was used to solve the optimization problem [41]. Here, we set the parameter opts.rFlag = 1, so that λ_1 and λ_2 are the ratios of the maximal sparse parameter, above which the sparse parameter could cause

the zero solution. To find the optimal sparsity of MFN for ASD diagnosis, we constructed MFN by varying the λ_1 and λ_2 values in specified ranges, where $\lambda_1 = \{2^{-1}, 2^{-2}, ..., 2^{-10}\}$ and $\lambda_2 = \{0.1, 0.2, ..., 1\}$, and evaluated the corresponding performance in terms of classification accuracy.

A schematic overview of MFN construction is shown in Fig. 1(a), where an example of the MFN and its incidence matrix (with *m* nodes, i.e., v_1 - v_m, rather than 358 for the real data) was also illustrated. Each row in the incidence matrix is the set of sparse coefficients from the linear regression model with the corresponding node as the target variable (labeled on the right side), with non-zero values being set to 1. A value of one suggests a relative robust relationship between the target region and all other regions included in the regression analysis, while a value of zero suggests a weak relationship. The asymmetrical MFN matrix, therefore, is a result of multiple regression process. For each subject, the binary values of the asymmetrical matrix were concatenated to form a feature vector with $358 \times (358-1) = 127,806$ elements, which was used as the input of feature selection. Notably, the asymmetric matrix does not reflect any causality [42], rather, it represents region-to-region similarity in terms of GM morphology.

2.4 Properties of the MFN

Although edges of MFN do not represent brain connectivity, we can treat the similarity matrix as a network. Here, we extracted three types of network properties, which reflect the local and global organizations of a network, as extra features that may potentially enhance the classification performance. Network properties were calculated using the Brain Connectivity Toolbox [43].

Clustering coefficient (CC) measures the local connective density of neighbors of a given node. The CC of node *i* is defined as the number of existing edges between neighbors of this node divided by all possible edges between this node and its neighbors [44], which is formulated as:

$$CC_i = \frac{1}{n}\sum_{i\in N} \frac{\sum_j \sum_h (e_{ij} + e_{ji})(e_{ih} + e_{hi})(e_{jh} + e_{hj})}{2K_i(K_i - 1) - \sum_j e_{ij} e_{ji}} \quad (2)$$

where e_{ij} is the edge from node *i* to node *j*, and *n* is the number of nodes.

Degree (K) measures the importance of nodes in the network, which is defined as the number of edges that are connecting to a specific node.

Global efficiency (GE) quantifies the efficiency of information transfer across the entire brain, formulated as:

$$GE = \frac{1}{n}\sum_{i\in N} \frac{\sum_{j\in N, j\neq i} (d_{ij}^{\rightarrow})^{-1}}{n-1} \quad (3)$$

where $d_{ij}^{\rightarrow}$ is the shortest path length from node *i* to node *j*.

2.5 Feature Selection and Group Discrimination

To generate a relative unbiased assessment of classification performance, we applied the leave-one-out cross-validation strategy with nested feature selection and classifier training only on training set of each interaction (see Fig. 1(b)). Here, we applied a two-step feature selection strategy to find a relative optimal feature subset. The first step of feature selection was utilized to roughly filter-out the features that are irrelevant for the categorization. We applied χ^2 test as a filter feature selection method for discrete features (MFN connection), and two sample t-test for continuous features (morphological features and network properties). Features with *p*-values exceeding 0.05 (uncorrected) were excluded. The selected features were then evaluated by linear SVM-based recursive feature elimination (SVM-RFE) [45] during the second step of feature selection. SVM-RFE is a backward feature elimination strategy that iteratively removes the features with the lowest discrimination performance as evaluated by SVM. We used the linear kernel to evaluate the importance of each feature with the ranking criterion as the square term of weight coefficients (w^2), calculated by $\mathbf{w} = \sum_k \alpha_k y_k \mathbf{x}_k$, where y_k and $\mathbf{x}_k$ is the class label and the n dimensional feature vector, of sample *k*, respectively; α is an index of support vector, corresponding samples of non-zero values in α are support vectors. Because the feature vector is multiplied by class label, a high discriminative feature should have a large value of $|w|$. In each interaction, the 500 lowest ranking features were removed when feature dimension was over 10,000; the step size was reduced to 50 for the last 10,000 features, 5 for the last 1,000 features, and 1 for the last 100 features. Because the dimensions of regional morphological features and network properties were small (358 features for each), only one step of feature selection, the SVM-RFE, was utilized in the classification procedures based on these features.

The two-step feature selection was conducted on all participants to evaluate the importance of each feature. Because each classifier might be trained by different features, utilization of the whole dataset enabled us to find features that most likely contributed to the discrimination between these two cohorts (TDC vs. ASD). Large absolute weight derived from SVM-RFE indicates the discriminative ability of a feature. Note that only connections with $p < 0.05$ (χ^2 test) were evaluated by SVM-RFE due to the two-step feature selection strategy. To investigate the driving regions that primarily contribute to the abnormal cortico-cortical similarity in ASD, we scored each brain region by summing up the absolute SVM-RFE weights of connections to this region. Regions with higher scores indicate these regions are more relevant to the discriminative connections and are key regions that responds more to the altered cortico-cortical relationship in ASD compared to the TDC.

2.6 Classification

The assessment of classification performance was conducted using the LIBSVM toolbox [46]. A nested five-fold cross validation was applied to optimize parameter C of

TABLE 2
COMPARISONS OF CLASSIFICATION PERFORMANCES BASED ON MORPHOLOGICAL FEATURES, NETWORK PROPERTIES, MFN CONNECTIONS, AND THE FEATURE COMBINATIONS

	Features	ACC (%)	SEN (%)	SPE (%)	AUC	P_{MFN}
Morphological Features	CT	62.60	60.00	65.15	0.59	0.0044
	SA	51.15	52.31	50.00	0.49	< 0.0001
	CV	64.12	61.54	66.67	0.67	0.0094
	LGI	60.31	55.38	65.15	0.60	0.0013
	SD	54.20	47.69	60.61	0.57	< 0.0001
	GH	51.91	49.23	54.55	0.50	< 0.0001
	CURV	58.78	60.00	57.58	0.59	0.0005
	MF	58.02	55.38	60.61	0.57	0.0003
	GM density	57.58	56.06	59.09	0.57	0.0003
Network Properties	CC	58.02	67.69	48.48	0.66	0.0003
	K	57.25	56.92	57.58	0.55	0.0002
	GE	50.38	100	0	-	< 0.0001
	NP	58.02	53.85	62.12	0.60	0.0003
MFN Connections	Connections	**78.63**	80.00	77.27	0.83	-
	Connections + MF	70.23	72.31	68.18	0.75	0.1193
	Connections + NP	71.76	76.92	66.67	0.74	0.1980
	Connections + MF + NP	78.63	75.38	81.82	0.85	1

MF = the combination of all morphological features; NP = the combination of all network properties; MFN = multi-feature-based network; ACC = accuracy; SEN = sensitivity; SPE = specificity; AUC = area under curve; P_{MFN} = compared the ACC obtained by each feature in relative to MFN by using χ^2 test.

the linear SVM classifier in the range of $\{2^{-8}, 2^{-7}, ..., 2^{8}\}$ on the training dataset of each cross validation process. The final classifier was trained based on the selected features and the parameter. We used accuracy, sensitivity, specificity, and area under the receiver operating characteristic curve (AUC) as the indices for the assessment. We utilized χ^2 test to determine the statistical significance in accuracy based on the different types and combinations of features.

2.7 Randomization Test

To examine the statistical significance of classification performance relative to random guessing, a randomization test was utilized, which generated the confidence interval (CI) of accuracy at chance level by repeating the entire cross-validation procedure for 500 times using randomly shuffled ASD and TDC labels. The real accuracy that exceed 95% CI was considered significantly different from chance level. We conducted the randomization test separately for each type of features.

3 RESULTS

3.1 Classification based on morphological features

Classification analyses showed the limited discriminative power in identifying patients with ASD from TDCs based on morphological measures (accuracies < 65%), which is consistent with previous findings from large heterogeneous samples [12, 14]. Classification accuracies and ROC curves of different classification analyses are shown in Fig. 2(a) and (b). Data smoothing and vertex-wised information did not further improve the classification performance (*ps* > 0.05, Table S1 and S2). Regional features extracted from unsmoothed data were, therefore, used for further analysis. The combination of all regional morphological features could not further improve the classification accuracy (58.02%) when compared to accuracies of

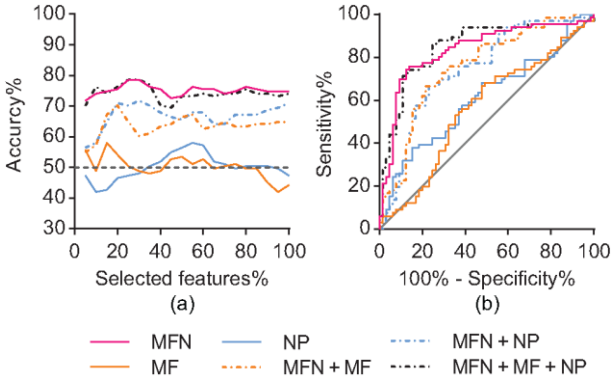

Fig. 2. Classification performances of different classification procedures. (a) Classification accuracies with varying proportion of enrolled features. MF is the combination of all morphological features; NP is the combination of all network properties. (b) ROC at the best classification performance.

using CT (62.60%), CV (64.12%), and LGI (60.31%) alone (Table 2). By utilizing the randomization test, we found that above-chance accuracy was only achieved by using CV (accuracy = 64.12%, $p < 0.05$), whereas other morphological measures and their combinations were indistinguishable from chance level (Fig. 3). Similar results were also observed with the voxel-based morphometry, which achieved accuracies of 57.58% by using regional GM density, with no significant improvement from chance level (Fig. 3).

3.2 Classification performance based on MFN connections

By varying parameters λ_1 and λ_2, the accuracy of MFN connections peaked at $\lambda_1 = 2^{-9}$ and $\lambda_2 = 0.7$, with the accuracy of 78.63%, AUC of 0.83 (Table 2 and Fig. 2), and a significant improvement relative to accuracies of morphological features (*ps* < 0.01, Table 2). Furthermore, the best classification performance was achieved by using only 25% of the top-ranked features that survived from the χ^2 test ($p < 0.05$), indicating that the marked diagnostic performance resulted from a small subset of features derived from a relative sparser network (Fig. 2(a)). Combining morphological features with MFN connections (MFN + MF) did not further enhance the classification performance, which only achieved 70.23% in accuracy with AUC of 0.75, though it performed better than using morphological features alone. Results from randomization test showed significant above-chance accuracies achieved by both MFN connection and the combination of MFN and morphological features ($p < 0.05$, Fig. 3). Results from single site analyses showed that the accuracies of SBL (92.37%), NYU (88.55%), and ISMMS (83.21%) were higher than the accuracy across all sites, whereas the accuracy of KUL was not (76.34%).

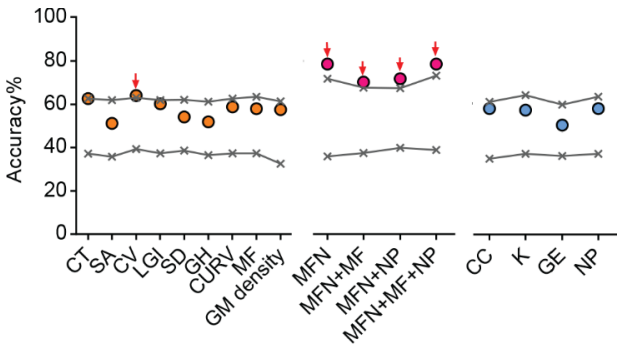

Fig. 3. Comparison of the classification accuracies of morphological features, MFN and their combinations, and network properties, with chance level. The grey lines with each point as a '×' represents the 5% and 95% CI of chance accuracy distribution estimated by randomization analysis on each type of features. Red arrows indicate significant above-chance accuracies (p < 0.05).

3.3 Discrimination of network properties

We employed network properties of the MFNs at the best-performing parameters ($\lambda_1 = 2^{-9}$, $\lambda_2 = 0.7$) as potential means for further improving the classification performance. However, the classification power of network properties and their combinations were similar as using some of the morphological features (accuracies < 60%, see Table 2), which were not statistically distinguishable from chance-level (Fig. 3). Moreover, these network properties provide limited supplementary information to the classifier beyond MFN connections (MFN + NP), which achieved only 71.76% in accuracy, with no further enhancement (Fig. 2(a) and Table 2). Although the classification performance that combined MFN, morphological features, and network properties together received significant improvement in accuracy (MFN + MF + NP, accuracy = 78.63%, $p < 0.05$), it still did not significantly exceed the performance of MFN alone.

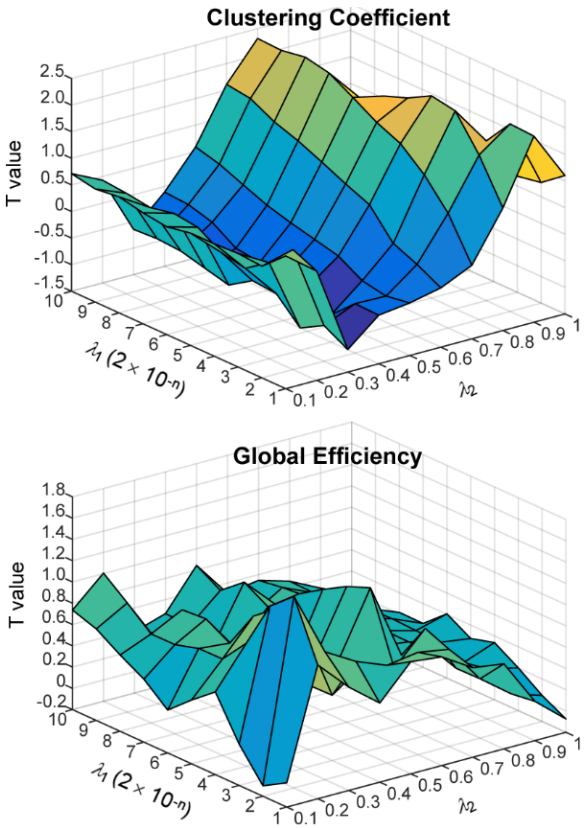

Fig. 4. Comparison of network properties between patients with ASD and the TDCs.

We further examined the difference in network properties by using statistical analysis. False discovery rate (FDR) was used for correcting the threshold of multiple comparisons. Results showed no significant differences in CC as well as in GE between the two cohorts (*qs* > 0.05, two sample t-test, FDR corrected), further supporting the argument that network properties have limited contribution to the discrimination. The T values of comparisons are shown in Fig. 4.

3.4 Discriminative connections and regions related to MFN discrimination

The top 30 discriminative anatomical connections with the highest absolute weights are shown in Fig. 5. We found that abnormal connections in ASD were mainly associated with the prefrontal cortex (e.g., Broadman area 9, 10, and medial prefrontal cortex), anterior cingulate gyrus, and areas in the parietal and occipital lobe (e.g., inferior parietal cortex, precuneus, and area V1). For example, abnormal connections were found between the left middle insula (MI) and left frontal eye field (FEF), left V1 area and right premotor eye field (PEF), and left 7P medial area (7Pm) and left Broadman area 45. In addition, connections with higher weights were mostly long-distance connections that linked anterior areas with middle and posterior areas of the brain. The abbreviations of all brain regions are shown in Table S3.

Brain regions with the top 5% scores, defined as the sum of absolute SVM-RFE weights of the connected links,

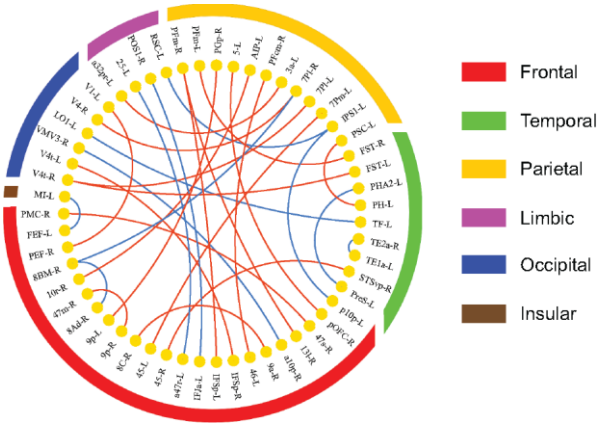

Fig. 5. The top 30 discriminative connections evaluated by two-step feature selection process. Red and blue edges indicate the increased and decreased proportion of connections in ASD, respectively. Six cerebral lobes are labeled with different colors.

are visualized in Fig. 6. The regions that are primarily responsible for the abnormalities in cortico-cortical relationship of ASD include, for example, the dorsal, medial and ventral prefrontal cortices (e.g., Broadman area 9, 8, and 47), right primary motor cortex (PMC), left primary visual cortex (V1), right supramarginal gyrus (area PFm), left precuneus (lateral area 7P), and left middle insula (MI).

4 Discussion

4.1 Limited diagnostic utility of the direct use of morphological measures for ASD classification

Our results showed limited discriminative ability when using only morphological measures derived from both surface-based and voxel-based morphometry in classifying individuals with ASD and TDCs. Poor classification accuracy indicates that morphological measures are mostly indistinguishable at the group level, suggesting the cerebral morphology may have limited diagnostic value of ASD. This is consistent with previous findings demonstrating low discriminative power of morphological measures in ASD classification [12, 14]. We speculated

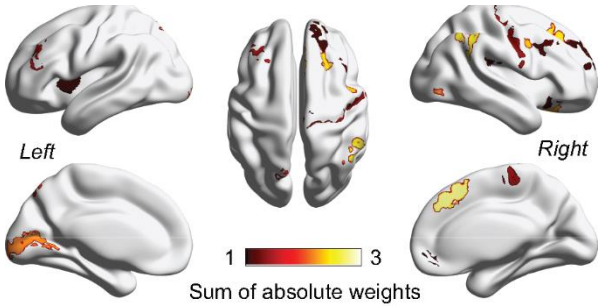

Fig. 6. The sagittal and axial views of top 5% brain regions that highly associated with discriminative connections. Color indicates the magnitude of sum of absolute weights of connections linked to the regions.

that the unsatisfactory classification performance may result from the reduced abnormalities in brain structures of adults with ASD [47, 48]: early overgrowth of morphological structures is compensated by accelerated neuronal atrophy in adulthood [49, 50]. In addition, the accuracy achieved by CV that significantly exceeded chance-level is consistent with the findings of higher discriminative power of CV on large sample size [14].

4.2 Cortico-cortical similarity captures critical abnormalities

Compared to morphological features, cortico-cortical similarity takes the relationship between the target region and other brain regions into account, which represents the nature of the cortical interplay. The significant improvement of classification performance based on MFN connections suggests that the relationships among cortical structures possess important information and could be utilized for diagnostic application of ASD.

Cortico-cortical similarity may be a more sensitive index to capture the coherent abnormalities among brain structures in ASD. Although the brain regions linked by discriminative connections have been previously reported to have significant GM alterations in ASD (e.g., anterior cingulate gyrus (ACG) [51], precuneus, and insula [52], superior temporal sulcus (STS) [53-55], V1 and inferior parietal lobule [56], lateral occipital cortex and paracentral area [57], and inferior and superior frontal gyri [10, 56]), no significant alterations were found in most of these areas in our previous VBM study conducted on the same dataset [10], e.g., we did not find significant GM changes in MI, ACC, and STS in this dataset, suggesting relatively less significant alterations in GM structures. Moreover, the limited classification performance of morphological measures suggests that the ASD-related structural changes are relatively undetectable. Based on the improved classification performance using MFN, we thus speculated that changes in structural similarity characterize cortical abnormalities in ASD. These changes were represented as increased differences in long-distance connections as reported in studies using other imaging modalities [58-61], suggesting ASD might affect large-scale cortico-cortical relationship all over the brain rather than the morphology of isolated brain regions.

There is evidence suggesting that the morphological similarities may partially mirror the functional alterations

[62]. For instance, significant reductions in CV and CV-based inter-regional correlation within prefrontal and temporal lobes are associated with the schizophrenia induced dissociation in fronto-temporal system [63]. ASD is known as associated with complex symptoms affecting multiple cognitive functions (e.g., sensory processing, emotional and cognitive functions, language, and social cognition) [1, 64-68], together with interregional communications associated with these functions [58, 69-72]. Here, the brain regions that were primarily associated with the altered connections were mostly in the aforementioned functional systems. Specifically, the ventromedial prefrontal cortex, insula, and precuneus are key regions for socio-emotional processing [73-78], and prefrontal cortex is also associated with language processing [79, 80] and cognitive control [67, 81, 82]; the V1 and V4 areas belong to the visual system [83, 84]; and PMC is the primary region of the motor system [85]. The high weights of these regions suggest their structures are altered in patients with ASD, which is consistent with ASD symptomatology, including abnormalities in social behavior [86, 87], socio-emotional processing [61, 88], language [89, 90], basic motor control [91] and gesture skills [92], visual-motion integration [93], and response to visual stimuli [94-96]. In addition, the discriminative pattern was different from our previous findings in Alzheimer's disease and mild cognitive impairment, in which the high-weight connections in classification were mostly related to the temporal lobe and fronto-temporal cortex [32] which have been reported to be primarily associated with disease progression [97-100]. Therefore, the cortico-cortical similarities among brain structures may represent the ASD-specific functional deficits and provide critical information for ASD diagnosis.

Although the MFN connections are informative for the classification of ASD, the network properties exhibited no (or limited) discriminative value, suggesting that the overall segregation (CC) and integration (GE) of morphological networks in patients with ASD are not abnormal. Although our previous MFN study [101], as well as other studies of morphological networks [102-104] indicated altered network properties (e.g., CC and characteristic path length) and small-word architecture, these studies mainly focused on neurodegenerative diseases (e.g., Alzheimer's disease) that are accompanied by evident GM atrophy. In the present study, because no distinct discrimination was found in various morphological measures between patients with ASD and TDCs, the connective differences that were mainly caused by structural abnormalities were relatively small, and therefore led to only slight changes in the overall organization of MFN.

4.3 Limitations

Although we have significantly enhanced the classification performance based on structural images, our resulting performance was only 78.63%, which is not high, and is consistent with some previous studies that demonstrated the limited diagnostic utility of morphological features for ASD diagnosis [12, 14]. However, other studies using structural images achieved marked performances (accuracies up to 90% by using CT, and accuracies up to 81% by using CV) in ASD classification [15, 17, 18]. The variability may be due to the differences in sample sizes, characteristics of participants (e.g., age and IQ), or scanners. For this analysis, we used a dataset from multiple centers. The performance of the classification for the cross-site sample (78.63%) was lower than for single site: SBL (92.37%), NYU (88.55%), and ISMMS (83.21%), but slightly higher than the performance of KUL (76.34%). Although comparisons between the classification performances of single site and across multiple sites was performed, replications on large independent samples would still be beneficial to examine the source of variance and the generalizability of the findings. The limited performance may also be resulted from the exclusion of subcortical tissues, as the construction of the MFN requires multiple morphological features in each brain region. Subcortical regions (e.g., amygdala and thalamus) were reported with significant CV alterations in patients with ASD [105-107] and significant above chance diagnostic accuracy for ASD [12]. The omission of these critical information may have negatively impacted the classification performance. Further studies may benefit from the inclusion of subcortical structures in the classification.

5 Conclusion

We utilized Elastic Network to quantify the cortico-cortical similarity based on 7 morphological features. The significant improvement of classification accuracy suggest that the cortico-cortical similarity is superior to morphological features in identifying high-functioning adults with ASD, and has potential application value in ASD diagnosis.

Acknowledgment

Funding: This work was supported by the National Key Basic Research and Development Program of China (grant number 2014CB744600, to B.H.), the National Natural Science Foundation of China (grant number 61632014, to BH, and grant number 81729001, to J.F.), and the Program of Beijing Municipal Science & Technology Commission (grant number Z171100000117005, to B.H.). This work was also supported in part by NIH grant R21 MH083164 and Simons Award 330704 (to J.F.), and grant and NSF IIS (grant number 1718802, to C.C.). **Conflicts of interest:** authors declare there is no conflict of interest in relation to this work. **Corresponding Author:** B. Hu (Email: bh@lzu.edu.cn) and J. Fan (Email: jin.fan@qc.cuny.edu).

References

[1] S. Baron-Cohen, "Theory of mind and autism: A fifteen year review," *Understanding other minds: Perspectives from developmental cognitive neuroscience,* vol. 2, pp. 3-20, 2000.

[2] A. P. Association, *Diagnostic and statistical manual of mental disorders (DSM-5®)*: American Psychiatric Pub, 2013.

[3] G. N. Soke, M. Maenner, D. Christensen, M. Kurzius-Spencer, and L. Schieve, "Brief Report: Estimated Prevalence of a

Community Diagnosis of Autism Spectrum Disorder by Age 4 Years in Children from Selected Areas in the United States in 2010: Evaluation of Birth Cohort Effects," *Journal of Autism and Developmental Disorders,* vol. 47, pp. 1917-1922, 2017.

[4] D. L. Christensen, D. A. Bilder, W. Zahorodny, S. Pettygrove, M. S. Durkin, R. T. Fitzgerald, *et al.*, "Prevalence and characteristics of autism spectrum disorder among 4-year-old children in the autism and developmental disabilities monitoring network," *Journal of Developmental & Behavioral Pediatrics,* vol. 37, pp. 1-8, 2016.

[5] C. f. D. Control and Prevention, "National diabetes statistics report: estimates of diabetes and its burden in the United States, 2014," *Atlanta, GA: US Department of Health and Human Services,* vol. 2014, 2014.

[6] C. Lord, S. Risi, L. Lambrecht, E. H. Cook, B. L. Leventhal, P. C. DiLavore, *et al.*, "The Autism Diagnostic Observation Schedule—Generic: A standard measure of social and communication deficits associated with the spectrum of autism," *Journal of autism and developmental disorders,* vol. 30, pp. 205-223, 2000.

[7] C. Lord, M. Rutter, and A. Le Couteur, "Autism Diagnostic Interview-Revised: a revised version of a diagnostic interview for caregivers of individuals with possible pervasive developmental disorders," *Journal of autism and developmental disorders,* vol. 24, pp. 659-685, 1994.

[8] C. Ecker, S. Y. Bookheimer, and D. G. Murphy, "Neuroimaging in autism spectrum disorder: brain structure and function across the lifespan," *The Lancet Neurology,* vol. 14, pp. 1121-1134, 2015.

[9] C. Ecker, C. Ginestet, Y. Feng, P. Johnston, M. V. Lombardo, M.-C. Lai, *et al.*, "Brain surface anatomy in adults with autism: the relationship between surface area, cortical thickness, and autistic symptoms," *Jama Psychiatry,* vol. 70, pp. 59-70, 2013.

[10] T. Eilam-Stock, T. Wu, A. Spagna, L. J. Egan, and J. Fan, "Neuroanatomical alterations in high-functioning adults with autism spectrum disorder," *Frontiers in neuroscience,* vol. 10, 2016.

[11] L. E. Libero, T. P. DeRamus, H. D. Deshpande, and R. K. Kana, "Surface-based morphometry of the cortical architecture of autism spectrum disorders: volume, thickness, area, and gyrification," *Neuropsychologia,* vol. 62, pp. 1-10, 2014.

[12] S. Haar, S. Berman, M. Behrmann, and I. Dinstein, "Anatomical abnormalities in autism?," *Cerebral Cortex,* vol. 26, pp. 1440-1452, 2014.

[13] J. A. Nielsen, B. A. Zielinski, P. T. Fletcher, A. L. Alexander, N. Lange, E. D. Bigler, *et al.*, "Multisite functional connectivity MRI classification of autism: ABIDE results," *Frontiers in human neuroscience,* vol. 7, 2013.

[14] G. J. Katuwal, N. D. Cahill, S. A. Baum, and A. M. Michael, "The predictive power of structural MRI in Autism diagnosis," in *Engineering in Medicine and Biology Society (EMBC), 2015 37th Annual International Conference of the IEEE*, 2015, pp. 4270-4273.

[15] C. Ecker, V. Rocha-Rego, P. Johnston, J. Mourao-Miranda, A. Marquand, E. M. Daly, *et al.*, "Investigating the predictive value of whole-brain structural MR scans in autism: a pattern classification approach," *Neuroimage,* vol. 49, pp. 44-56, 2010.

[16] L. Q. Uddin, V. Menon, C. B. Young, S. Ryali, T. Chen, A. Khouzam, *et al.*, "Multivariate searchlight classification of structural magnetic resonance imaging in children and adolescents with autism," *Biological psychiatry,* vol. 70, pp. 833-841, 2011.

[17] C. Ecker, A. Marquand, J. Mourão-Miranda, P. Johnston, E. M. Daly, M. J. Brammer, *et al.*, "Describing the brain in autism in five dimensions—magnetic resonance imaging-assisted diagnosis of autism spectrum disorder using a multiparameter classification approach," *Journal of Neuroscience,* vol. 30, pp. 10612-10623, 2010.

[18] Y. Jiao, R. Chen, X. Ke, K. Chu, Z. Lu, and E. H. Herskovits, "Predictive models of autism spectrum disorder based on brain regional cortical thickness," *Neuroimage,* vol. 50, pp. 589-599, 2010.

[19] C. Y. Wee, L. Wang, F. Shi, P. T. Yap, and D. Shen, "Diagnosis of autism spectrum disorders using regional and interregional morphological features," *Human brain mapping,* vol. 35, pp. 3414-3430, 2014.

[20] W. Zheng, Z. Yao, B. Hu, X. Gao, H. Cai, and P. Moore, "Novel Cortical Thickness Pattern for Accurate Detection of Alzheimer's Disease," *Journal of Alzheimer's Disease,* vol. 48, pp. 995-1008, 2015.

[21] C. Y. Wee, P. T. Yap, and D. Shen, "Prediction of Alzheimer's disease and mild cognitive impairment using cortical morphological patterns," *Hum Brain Mapp,* vol. 34, pp. 3411-25, Dec 2013.

[22] M. Saggar, S. H. Hosseini, J. L. Bruno, E.-M. Quintin, M. M. Raman, S. R. Kesler, *et al.*, "Estimating individual contribution from group-based structural correlation networks," *Neuroimage,* vol. 120, pp. 274-284, 2015.

[23] H. Zou and T. Hastie, "Regularization and variable selection via the elastic net," *Journal of the Royal Statistical Society: Series B (Statistical Methodology),* vol. 67, pp. 301-320, 2005.

[24] B. Fischl and A. M. Dale, "Measuring the thickness of the human cerebral cortex from magnetic resonance images," *Proceedings of the National Academy of Sciences,* vol. 97, pp. 11050-11055, 2000.

[25] M. Schaer, M. B. Cuadra, L. Tamarit, F. Lazeyras, S. Eliez, and J. P. Thiran, "A surface-based approach to quantify local cortical gyrification," *IEEE Trans Med Imaging,* vol. 27, pp. 161-70, Feb 2008.

[26] J. Rogers, P. Kochunov, J. Lancaster, W. Shelledy, D. Glahn, J. Blangero, *et al.*, "Heritability of brain volume, surface area and shape: an MRI study in an extended pedigree of baboons," *Human brain mapping,* vol. 28, pp. 576-583, 2007.

[27] C. Destrieux, B. Fischl, A. Dale, and E. Halgren, "Automatic parcellation of human cortical gyri and sulci using standard anatomical nomenclature," *Neuroimage,* vol. 53, pp. 1-15, 2010.

[28] B. Fischl, M. I. Sereno, and A. M. Dale, "Cortical surface-based analysis: II: Inflation, flattening, and a surface-based coordinate system," *Neuroimage,* vol. 9, pp. 195-207, 1999.

[29] M. Schaer, M. B. Cuadra, N. Schmansky, B. Fischl, J. P. Thiran, and S. Eliez, "How to measure cortical folding from MR images: a step-by-step tutorial to compute local gyrification index," *J Vis Exp,* p. e3417, 2012.

[30] N. Meinshausen and P. Bühlmann, "High-dimensional graphs and variable selection with the lasso," *The annals of statistics,* pp. 1436-1462, 2006.

[31] S. Ryali, T. Chen, K. Supekar, and V. Menon, "Estimation of functional connectivity in fMRI data using stability selection-

based sparse partial correlation with elastic net penalty," *NeuroImage,* vol. 59, pp. 3852-3861, 2012.

[32] W. Zheng, Z. Yao, Y. Xie, J. Fan, and B. Hu, "Identification of Alzheimer's disease and mild cognitive impairment using networks constructed based on multiple morphological brain features," *Biological Psychiatry: Cognitive Neuroscience and Neuroimaging,* 2018.

[33] C. Cortes and V. Vapnik, "Support-vector networks," *Machine learning,* vol. 20, pp. 273-297, 1995.

[34] F. Ségonne, A. M. Dale, E. Busa, M. Glessner, D. Salat, H. K. Hahn, *et al.*, "A hybrid approach to the skull stripping problem in MRI," *Neuroimage,* vol. 22, pp. 1060-1075, 2004.

[35] A. M. Dale, B. Fischl, and M. I. Sereno, "Cortical surface-based analysis: I. Segmentation and surface reconstruction," *Neuroimage,* vol. 9, pp. 179-194, 1999.

[36] B. Fischl, A. Liu, and A. M. Dale, "Automated manifold surgery: constructing geometrically accurate and topologically correct models of the human cerebral cortex," *IEEE Trans Med Imaging,* vol. 20, pp. 70-80, Jan 2001.

[37] J. Ashburner and K. J. Friston, "Unified segmentation," *Neuroimage,* vol. 26, pp. 839-851, 2005.

[38] J. Ashburner, "A fast diffeomorphic image registration algorithm," *Neuroimage,* vol. 38, pp. 95-113, 2007.

[39] M. F. Glasser, T. S. Coalson, E. C. Robinson, C. D. Hacker, J. Harwell, E. Yacoub, *et al.*, "A multi-modal parcellation of human cerebral cortex," *Nature,* vol. 536, pp. 171-178, 2016.

[40] R. Tibshirani, "Regression shrinkage and selection via the lasso," *Journal of the Royal Statistical Society. Series B (Methodological),* pp. 267-288, 1996.

[41] J. Liu, S. Ji, and J. Ye, "SLEP: Sparse learning with efficient projections," *Arizona State University,* vol. 6, p. 7, 2009.

[42] K. Friston, "Causal modelling and brain connectivity in functional magnetic resonance imaging," *PLoS biol,* vol. 7, p. e1000033, 2009.

[43] M. Rubinov and O. Sporns, "Complex network measures of brain connectivity: uses and interpretations," *Neuroimage,* vol. 52, pp. 1059-69, Sep 2010.

[44] G. Fagiolo, "Clustering in complex directed networks," *Physical Review E,* vol. 76, p. 026107, 08/16/ 2007.

[45] I. Guyon, J. Weston, S. Barnhill, and V. Vapnik, "Gene selection for cancer classification using support vector machines," *Machine learning,* vol. 46, pp. 389-422, 2002.

[46] C.-C. Chang and C.-J. Lin, "LIBSVM: a library for support vector machines," *ACM Transactions on Intelligent Systems and Technology (TIST),* vol. 2, p. 27, 2011.

[47] E. Redcay and E. Courchesne, "When is the brain enlarged in autism? A meta-analysis of all brain size reports," *Biological psychiatry,* vol. 58, pp. 1-9, 2005.

[48] E. Courchesne, K. Pierce, C. M. Schumann, E. Redcay, J. A. Buckwalter, D. P. Kennedy, *et al.*, "Mapping early brain development in autism," *Neuron,* vol. 56, pp. 399-413, 2007.

[49] E. Courchesne, K. Campbell, and S. Solso, "Brain growth across the life span in autism: age-specific changes in anatomical pathology," *Brain research,* vol. 1380, pp. 138-145, 2011.

[50] N. Lange, B. G. Travers, E. D. Bigler, M. B. Prigge, A. L. Froehlich, J. A. Nielsen, *et al.*, "Longitudinal volumetric brain changes in autism spectrum disorder ages 6–35 years," *Autism Research,* vol. 8, pp. 82-93, 2015.

[51] G. D. Waiter, J. H. Williams, A. D. Murray, A. Gilchrist, D. I. Perrett, and A. Whiten, "A voxel-based investigation of brain structure in male adolescents with autistic spectrum disorder," *Neuroimage,* vol. 22, pp. 619-625, 2004.

[52] F. Cauda, E. Geda, K. Sacco, F. D'agata, S. Duca, G. Geminiani, *et al.*, "Grey matter abnormality in autism spectrum disorder: an activation likelihood estimation meta-analysis study," *J Neurol Neurosurg Psychiatry,* vol. 82, pp. 1304-1313, 2011.

[53] E. Greimel, B. Nehrkorn, M. Schulte-Rüther, G. R. Fink, T. Nickl-Jockschat, B. Herpertz-Dahlmann, *et al.*, "Changes in grey matter development in autism spectrum disorder," *Brain Structure and Function,* vol. 218, pp. 929-942, 2013.

[54] N. Boddaert, N. Chabane, H. Gervais, C. Good, M. Bourgeois, M. Plumet, *et al.*, "Superior temporal sulcus anatomical abnormalities in childhood autism: a voxel-based morphometry MRI study," *Neuroimage,* vol. 23, pp. 364-369, 2004.

[55] M. Zilbovicius, I. Meresse, N. Chabane, F. Brunelle, Y. Samson, and N. Boddaert, "Autism, the superior temporal sulcus and social perception," *Trends in neurosciences,* vol. 29, pp. 359-366, 2006.

[56] K. L. Hyde, F. Samson, A. C. Evans, and L. Mottron, "Neuroanatomical differences in brain areas implicated in perceptual and other core features of autism revealed by cortical thickness analysis and voxel‐based morphometry," *Human brain mapping,* vol. 31, pp. 556-566, 2010.

[57] T. Nickl‐Jockschat, U. Habel, T. Maria Michel, J. Manning, A. R. Laird, P. T. Fox, *et al.*, "Brain structure anomalies in autism spectrum disorder—a meta‐analysis of VBM studies using anatomic likelihood estimation," *Human brain mapping,* vol. 33, pp. 1470-1489, 2012.

[58] P. Barttfeld, B. Wicker, S. Cukier, S. Navarta, S. Lew, and M. Sigman, "A big-world network in ASD: dynamical connectivity analysis reflects a deficit in long-range connections and an excess of short-range connections," *Neuropsychologia,* vol. 49, pp. 254-263, 2011.

[59] P. Rane, D. Cochran, S. M. Hodge, C. Haselgrove, D. Kennedy, and J. A. Frazier, "Connectivity in autism: A review of MRI connectivity studies," *Harvard review of psychiatry,* vol. 23, p. 223, 2015.

[60] R. K. Kana, L. E. Libero, and M. S. Moore, "Disrupted cortical connectivity theory as an explanatory model for autism spectrum disorders," *Physics of life reviews,* vol. 8, pp. 410-437, 2011.

[61] S. H. Ameis, J. Fan, C. Rockel, A. N. Voineskos, N. J. Lobaugh, L. Soorya, *et al.*, "Impaired structural connectivity of socio-emotional circuits in autism spectrum disorders: a diffusion tensor imaging study," *PloS one,* vol. 6, p. e28044, 2011.

[62] A. C. Evans, "Networks of anatomical covariance," *Neuroimage,* vol. 80, pp. 489-504, 2013.

[63] P. Woodruff, I. Wright, N. Shuriquie, H. Russouw, T. Rushe, R. Howard, *et al.*, "Structural brain abnormalities in male schizophrenics reflect fronto-temporal dissociation," *Psychological medicine,* vol. 27, pp. 1257-1266, 1997.

[64] G. Allen and E. Courchesne, "Differential effects of developmental cerebellar abnormality on cognitive and motor functions in the cerebellum: an fMRI study of autism," *American Journal of Psychiatry,* vol. 160, pp. 262-273, 2003.

[65] L. T. Eyler, K. Pierce, and E. Courchesne, "A failure of left

temporal cortex to specialize for language is an early emerging and fundamental property of autism," *Brain,* vol. 135, pp. 949-960, 2012.

[66] J. Fan, "Attentional network deficits in autism spectrum disorders," *The neuroscience of autism spectrum disorders,* pp. 281-288, 2012.

[67] M.-A. Mackie and J. Fan, "Functional neuroimaging of deficits in cognitive control," in *Executive Functions in Health and Disease*, ed: Elsevier, 2017, pp. 249-300.

[68] W. Perry, A. Minassian, B. Lopez, L. Maron, and A. Lincoln, "Sensorimotor gating deficits in adults with autism," *Biological psychiatry,* vol. 61, pp. 482-486, 2007.

[69] M. E. Vissers, M. X. Cohen, and H. M. Geurts, "Brain connectivity and high functioning autism: a promising path of research that needs refined models, methodological convergence, and stronger behavioral links," *Neuroscience & Biobehavioral Reviews,* vol. 36, pp. 604-625, 2012.

[70] S. Wass, "Distortions and disconnections: disrupted brain connectivity in autism," *Brain and cognition,* vol. 75, pp. 18-28, 2011.

[71] B. E. Yerys, J. D. Herrington, T. D. Satterthwaite, L. Guy, R. T. Schultz, and D. S. Bassett, "Globally weaker and topologically different: resting-state connectivity in youth with autism," *Molecular autism,* vol. 8, p. 39, 2017.

[72] T. Eilam-Stock, P. Xu, M. Cao, X. Gu, N. T. Van Dam, E. Anagnostou, *et al.*, "Abnormal autonomic and associated brain activities during rest in autism spectrum disorder," *Brain,* vol. 137, pp. 153-171, 2014.

[73] C. D. Frith and U. Frith, "Interacting minds--a biological basis," *Science,* vol. 286, pp. 1692-1695, 1999.

[74] H. L. Gallagher and C. D. Frith, "Functional imaging of 'theory of mind'," *Trends in cognitive sciences,* vol. 7, pp. 77-83, 2003.

[75] Y.-T. Fan, C. Chen, S.-C. Chen, J. Decety, and Y. Cheng, "Empathic arousal and social understanding in individuals with autism: evidence from fMRI and ERP measurements," *Social Cognitive and Affective Neuroscience,* vol. 9, pp. 1203-1213, 2013.

[76] D. M. Amodio and C. D. Frith, "Meeting of minds: the medial frontal cortex and social cognition," *Nature reviews. Neuroscience,* vol. 7, p. 268, 2006.

[77] X. Gu, P. R. Hof, K. J. Friston, and J. Fan, "Anterior insular cortex and emotional awareness," *Journal of Comparative Neurology,* vol. 521, pp. 3371-3388, 2013.

[78] A. Spagna, A. J. Dufford, Q. Wu, T. Wu, W. Zheng, E. E. Coons, *et al.*, "Gray matter volume of the anterior insular cortex and social networking," *Journal of Comparative Neurology,* vol. 526, pp. 1183-1194, 2018.

[79] A. D. Friederici, "The brain basis of language processing: from structure to function," *Physiological reviews,* vol. 91, pp. 1357-1392, 2011.

[80] F. Jessen, M. Erb, U. Klose, M. Lotze, W. Grodd, and R. Heun, "Activation of human language processing brain regions after the presentation of random letter strings demonstrated with event-related functional magnetic resonance imaging," *Neuroscience Letters,* vol. 270, pp. 13-16, 1999.

[81] J. Fan, N. T. Van Dam, X. Gu, X. Liu, H. Wang, C. Y. Tang, *et al.*, "Quantitative characterization of functional anatomical contributions to cognitive control under uncertainty," *Journal of cognitive neuroscience,* vol. 26, pp. 1490-1506, 2014.

[82] T. Wu, A. J. Dufford, L. J. Egan, M.-A. Mackie, C. Chen, C. Yuan, *et al.*, "Hick–Hyman Law is Mediated by the Cognitive Control Network in the Brain," *Cerebral Cortex,* pp. 1-16, 2017.

[83] S. Pitzalis, M. I. Sereno, G. Committeri, P. Fattori, G. Galati, F. Patria, *et al.*, "Human V6: the medial motion area," *Cerebral Cortex,* vol. 20, pp. 411-424, 2009.

[84] M. J. Arcaro, S. A. McMains, B. D. Singer, and S. Kastner, "Retinotopic organization of human ventral visual cortex," *Journal of neuroscience,* vol. 29, pp. 10638-10652, 2009.

[85] G. Rizzolatti and G. Luppino, "The cortical motor system," *Neuron,* vol. 31, pp. 889-901, 2001.

[86] S. W. White, K. Keonig, and L. Scahill, "Social skills development in children with autism spectrum disorders: A review of the intervention research," *Journal of autism and developmental disorders,* vol. 37, pp. 1858-1868, 2007.

[87] C. Kasari, J. Locke, A. Gulsrud, and E. Rotheram-Fuller, "Social networks and friendships at school: Comparing children with and without ASD," *Journal of autism and developmental disorders,* vol. 41, pp. 533-544, 2011.

[88] B. Wicker, P. Fonlupt, B. Hubert, C. Tardif, B. Gepner, and C. Deruelle, "Abnormal cerebral effective connectivity during explicit emotional processing in adults with autism spectrum disorder," *Social cognitive and affective neuroscience,* vol. 3, pp. 135-143, 2008.

[89] H. Tager - Flusberg, R. Paul, and C. Lord, "Language and communication in autism," *Handbook of Autism and Pervasive Developmental Disorders, Volume 1, Third Edition,* pp. 335-364, 2005.

[90] H. Tager-Flusberg, "Language impairments in children with complex neurodevelopmental disorders: The case of autism," *Language competence across populations: Toward a definition of specific language impairment,* pp. 297-321, 2003.

[91] E. M. Jansiewicz, M. C. Goldberg, C. J. Newschaffer, M. B. Denckla, R. Landa, and S. H. Mostofsky, "Motor signs distinguish children with high functioning autism and Asperger's syndrome from controls," *Journal of autism and developmental disorders,* vol. 36, pp. 613-621, 2006.

[92] S. H. Mostofsky, P. Dubey, V. K. Jerath, E. M. Jansiewicz, M. C. Goldberg, and M. B. Denckla, "Developmental dyspraxia is not limited to imitation in children with autism spectrum disorders," *Journal of the International Neuropsychological Society,* vol. 12, pp. 314-326, 2006.

[93] B. Gepner and D. Mestre, "Rapid visual-motion integration deficit in autism," *Trends in Cognitive Sciences,* vol. 6, p. 455, 2002.

[94] K. A. Pelphrey, N. J. Sasson, J. S. Reznick, G. Paul, B. D. Goldman, and J. Piven, "Visual scanning of faces in autism," *Journal of autism and developmental disorders,* vol. 32, pp. 249-261, 2002.

[95] J. A. Wainwright-Sharp and S. E. Bryson, "Visual orienting deficits in high-functioning people with autism," *Journal of Autism and Developmental disorders,* vol. 23, pp. 1-13, 1993.

[96] C. E. Robertson, C. Thomas, D. J. Kravitz, G. L. Wallace, S. Baron-Cohen, A. Martin, *et al.*, "Global motion perception deficits in autism are reflected as early as primary visual cortex," *Brain,* vol. 137, pp. 2588-2599, 2014.

[97] G. Chételat, B. Desgranges, B. Landeau, F. Mezenge, J. Poline, V. de La Sayette, *et al.*, "Direct voxel-based comparison between grey matter hypometabolism and atrophy in Alzheimer's

disease," *Brain,* vol. 131, pp. 60-71, 2008.

[98] J. Baron, G. Chetelat, B. Desgranges, G. Perchey, B. Landeau, V. De La Sayette, *et al.*, "In vivo mapping of gray matter loss with voxel-based morphometry in mild Alzheimer's disease," *Neuroimage,* vol. 14, pp. 298-309, 2001.

[99] G. Frisoni, C. Testa, A. Zorzan, F. Sabattoli, A. Beltramello, H. Soininen, *et al.*, "Detection of grey matter loss in mild Alzheimer's disease with voxel based morphometry," *Journal of Neurology, Neurosurgery & Psychiatry,* vol. 73, pp. 657-664, 2002.

[100] C. D. Good, R. I. Scahill, N. C. Fox, J. Ashburner, K. J. Friston, D. Chan, *et al.*, "Automatic differentiation of anatomical patterns in the human brain: validation with studies of degenerative dementias," *Neuroimage,* vol. 17, pp. 29-46, 2002.

[101] W. Zheng, Z. Yao, Y. Xie, J. Fan, and B. Hu, "Identification of Alzheimer's disease and mild cognitive impairment using networks constructed based on multiple morphological brain features," *under review*.

[102] Y. He, Z. Chen, and A. Evans, "Structural insights into aberrant topological patterns of large-scale cortical networks in Alzheimer's disease," *The Journal of neuroscience,* vol. 28, pp. 4756-4766, Apr 30 2008.

[103] Z. Yao, Y. Zhang, L. Lin, Y. Zhou, C. Xu, T. Jiang, *et al.*, "Abnormal cortical networks in mild cognitive impairment and Alzheimer's disease," *PLoS computational biology,* vol. 6, p. e1001006, 2010.

[104] J. B. Pereira, M. Mijalkov, E. Kakaei, P. Mecocci, B. Vellas, M. Tsolaki, *et al.*, "Disrupted Network Topology in Patients with Stable and Progressive Mild Cognitive Impairment and Alzheimer's Disease," *Cerebral Cortex,* p. bhw128, 2016.

[105] R. Jacobson, A. Le Couteur, P. Howlin, and M. Rutter, "Selective subcortical abnormalities in autism," *Psychological medicine,* vol. 18, pp. 39-48, 1988.

[106] M. Bellani, S. Calderoni, F. Muratori, and P. Brambilla, "Brain anatomy of autism spectrum disorders II. Focus on amygdala," *Epidemiology and psychiatric sciences,* vol. 22, pp. 309-312, 2013.

[107] R. Tamura, H. Kitamura, T. Endo, N. Hasegawa, and T. Someya, "Reduced thalamic volume observed across different subgroups of autism spectrum disorders," *Psychiatry Research: Neuroimaging,* vol. 184, pp. 186-188, 2010.

W. Zheng completed his B.A. in Electronic Information Science and Technology from Shenyang University, and M.A. in Circuit and System from Lanzhou University, respectively. He is now a PhD student at Lanzhou University. His research interests include machine learning and brain image analysis.

T. Eilam-Stock received her B.A. in Psychology and Music from the Hebrew University in Jerusalem and the Jerusalem Academy of Music and Dance, Israel. Tehila then completed her M.A. in Psychology at The City University of New York (CUNY), Hunter College. Tehila is received her doctoral degree of Clinical Neuropsychology at Queens College and the CUNY Graduate Center. Tehila studies the neural correlates of socio-emotional processing and its relationship to autonomic activity during task and at rest, in neurotypical individuals, as well as in individuals with Autism Spectrum Disorder.

T. Wu Tingting Wu received her B.S. in Biological Science from Nanjing University in 2007. She received her PhD in Cognitive Neuroscience in Beijing Normal University in 2013. She then moved to New York to work as a postdoctoral scholar in the Cognitive Neuroscience Lab. Her current research interests focus on cognitive control, including the neural mechanism and computational modeling.

A. Spagna is a visiting doctoral student from the Department of Psychology, Sapienza, University of Rome. In 2010 He received his Master's degree in Cognitive Neuropsychology at Sapienza and he is currently a graduate student in the Cognitive Psychology, Psychophysiology and Personality Ph.D. Program. Alfredo's current focus is on studying the efficiency and interactions of the attentional networks in visual and auditory modality using the Attention Network Test, and assessing the existence of a supramodal mechanism through which attentional resources are allocated to different environments.

C. Chen is an assistant professor of Biomedical Informatics at Stony Brook University, United States. He received his B.S from Peking University, and completed his Ph.D program at Rensselaer Polytechnic Institute, USA. His research Interests include machine learning, topological data analysis, and biomedical image analysis.

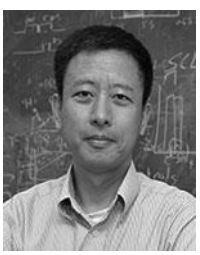

J. Fan is a Professor of Psychology at Queens College, the City University of New York. He received his PhD from New York University, followed by post-doctoral training at Weill Medical College of Cornell University. Before joining Queens College, he worked at Mount Sinai School of Medicine as an assistant professor of neuroscience and psychiatry. Dr. Fan's research focuses on human attentional processes conceptualized as a system of anatomical areas forming specialized networks. Through independent research and collaboration, he has conducted behavioral, developmental, and patient-based studies using functional magnetic resonance imaging, event related potentials, genetics, and computational modeling to investigate the anatomy, circuitry, pathology, and development of attentional networks. Dr. Fan has expertise in cognitive and affective neuroscience, specifically various neuroimaging methods.

B. Hu, Ph.D., Professor, Dean of the School of Information Science & Engineering at Lanzhou University, China, IET Fellow. His research interests include using computational approaches to decode emotion, mind and behavior. He has published over 200 papers in peer-reviewed journals, conferences, and book chapters.